

Experimental Study and Mathematical Modelling of Straw Co-Firing with Propane

Inesa Barmina^a, Antons Kolmickovs^{a,*}, Raimonds Valdmanis^a, Maija Zake^a, Harijs Kalis^b, Maxims Marinaki^b

^a Institute of Physics, University of Latvia, 32 Miera Street, Salaspils-1, LV-2169, Latvia

^b Institute of Mathematics and Informatics, University of Latvia, 29 Raina boulevard, Riga, LV-1459, Latvia
antons.kolmickovs@lu.lv

The goal of this study is to provide a more effective use of wheat straw for energy production by co-firing it with a gaseous fossil fuel – propane. The study includes experimental work and mathematical modelling of the processes developing at co-firing – the influence of the additional heat supply on the thermal decomposition of straw, on the formation, ignition and combustion of volatiles, on the heat output from the device and on the flue gas composition. Experimental results give evidence that the straw co-firing with propane enhances the thermal decomposition of wheat straw pellets providing so faster formation, ignition and more complete burnout of the volatiles. By increasing the propane supply into the device up to 0.6 l/min (\approx 0.9 kW), the volume fractions of H₂ and CO at the gasifier outlet increase by about 36 % and 45 %, respectively. The improved combustion of the volatiles downstream the combustor results in correlating increase of the temperature in the flame reaction zone (from 1,060 K up to 1,200 K), hence, increasing the heat power of the device by about 44 %. In addition, the wheat straw co-firing with propane improves the flue gas composition, decreasing the mass fraction of unburned CO in the products from 1.800 ppm to 800 ppm, H₂ from 250 ppm to 40 ppm and the mass fraction of the hazardous NO_x emission from 400 ppm to 250 ppm. A mathematical model of the combustion dynamics at co-firing straw with propane has been developed using MATLAB, considering the variations of the additional heat energy supply from the propane flame flow.

1. Introduction

The main goal of the current research refers to the EU 2030 targets to reduce the overall greenhouse gas (GHG) emissions by 40 %, to increase the energy production efficiency and the utilization of renewable energy sources by 27 %, thus minimizing the effect of heat producers on the GHG emissions and global warming. In this context, the use of different types of agriculture and harvesting residues for the energy production is severe (EU Commission, 2018). Although there is a debate concerning the agriculture residue life-cycle emissions, some plant biomasses (wheat straw) are accepted as a CO₂ neutral fuel that does not contribute to global warming. Despite this, straw is a problematic fuel due to the high nitrogen and ash contents, with the low carbon and hydrogen contents (Vassilev et al., 2012), determining the low heating value of straw. In addition, the use of straw for heat production can cause problems related to slagging, corrosion (Veijonen et al., 2003), the increased emission of both NO_x and CO, and also causes the formation of ash agglomerates (Jandačka et al., 2012). To minimize the negative effects, the co-firing of straw with wood (Nordgren et al., 2013), coal (Wang et al., 2014), peat (Barmina et al., 2018a) or with natural gas (Agbor, 2015) was studied considering the feasibility of the straw co-firing to improve the utilization of straw for the combustion processes. Nowadays the co-firing of biomass with fossil (Nussbaumer, 2003) and renewable (Basu, 2018) fuels has become an ordinary and mature technology for energy production. However, the efficiency of heat production and the composition of flue gases are highly influenced by the specific properties of the fuel components and additional studies are needed to assess their impact on the main biomass/propane co-firing characteristics and on the composition of combustion products.

2. Experimental

Effects of the wheat straw gasification/co-firing with propane were studied using a batch-size pilot device ($P_{0, av} \approx 1.5$ kW) consisting of a fixed bed discrete portion biomass gasifier, a combustion chamber and a propane flame burner (P_{prop} varied from ~ 0.5 kW up to ~ 0.9 kW). To assess the effect of additional heat supply on the thermo-chemical conversion of straw biomass when co-firing it with propane, complex measurements of the main gasification and combustion characteristics were carried out. They include measurements of the weight loss rate of the biomass layer (dm/dt), the composition of volatiles entering the combustor, the flame temperature, the heat output from the device, the total produced heat energy per mass of burned solid mass and the flue gas composition. The methodology of experiments is described in detail in (Barmina et al., 2018a; 2018b).

3. Results and discussion

As follows from the DTA and DTG studies (Barmina et al., 2018a), the thermo-chemical conversion of wheat straw in an oxidative atmosphere (air) resulted in formation of main weight loss rate and temperature peaks at around $T = 560$ K and 710 K. The formation of the first peak refers to the thermal decomposition of hemicellulose and lignin which are responsible for the emission of: CO_2 mainly at decarboxylation of hemicellulose, CO at decarbonylation of cellulose and light hydrocarbons, such as C_2H_2 and C_2H_4 , and CH_4 and H_2 , mainly due to the recombination and reduction processes. The formation of lignocellulosic char is accompanied by the devolatilization processes – by CO , CO_2 and H_2 emission due to this char surface red-ox reactions (Yang et al., 2007).

When co-firing straw pellets with gas, propane plays a significant role in enhancing the biomass heating and dewatering processes. The results of the experimental study suggest the most effective thermal decomposition of straw pellets to take place at the primary pre-combustion stage ($t = 160 - 600$ s). During this stage, an increase of the additional heat input up to 0.9 kW (by the propane flame flow) into the device ensures the enhanced thermal decomposition of wheat straw by increasing the average weight loss rate of the pelletized biomass from 0.027 g/s to 0.062 g/s (Figure 1a). The time-dependent study of the thermal decomposition of the wheat straw pellets under different co-firing regimes showed an increase of the weight loss rate at 300 s and at around 700 s up to 0.08 g/s and to 0.15 g/s, correspondingly (Figure 1b). The effect of the additional heat input on the biomass weight loss rate gradually decreased after $t > 600$ s when the layer of the pelletized biomass went down below the propane flame inlet nozzle. Further, at the biomass self-sustaining combustion stage, the propane flame flow predominately advances the burnout of volatiles emitted by the biomass, thus the effect on the biomass weight loss rate was reduced.

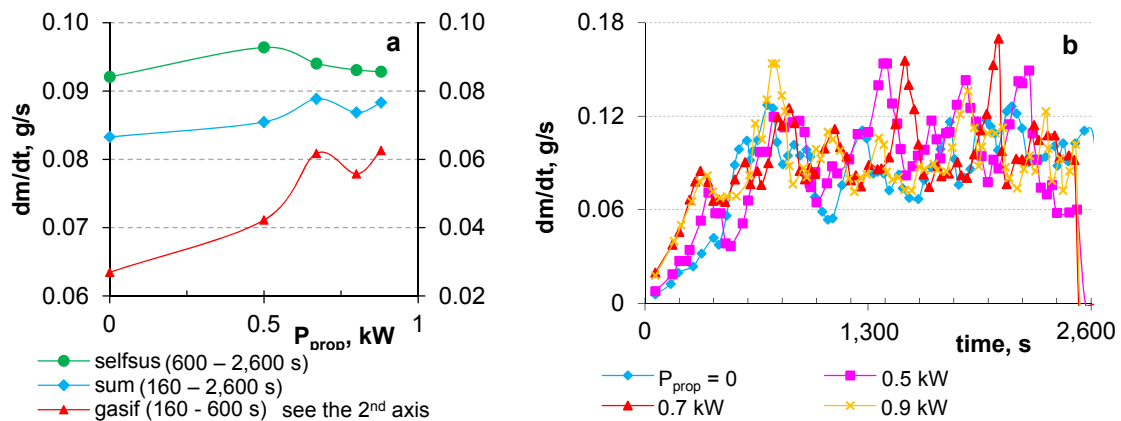


Figure 1: The effect of additional heat input on the averaged values of biomass weight loss rate (a) and on the time-dependent variations of the weight loss (b) during wheat straw / propane co-firing.

The time-dependent variations of the volatiles release (CO , H_2) presume the development of a two-step process of wheat straw thermal decomposition responsible for the formation of two peak values of CO at about 1,000 – 1,200 s and at 1,400 – 2,000 s. When increasing the heat input up to 0.9 kW, the first peak of the CO formation kinetics rapidly reached 86 g/m³ (from 58 g/m³) and slightly shifted from $\sim 1,200$ s to $\sim 1,000$ s time. The second CO formation peak demonstrates a more pronounced and faster growth if compared to the first peak: the peak value of the CO average volume fraction at the outlet of the gasifier

increased from 38 g/m^3 up to 75 g/m^3 and shifted from 2,000 s to 1,400 s (at $P_{\text{prop}} \approx 0.9 \text{ kW}$), thus indicating a faster oxidation of the straw lignocellulosic char (Figure 2a). As follows from Figure 2b, the additional heat supply from the propane flame flow enhances the thermal decomposition of holocellulose. As a result, the average values of C_2H_2 and C_2H_4 IR absorption increase when increasing the propane supply, which correlates with the weight loss rate increase during the primary stage of the flame formation (Figure 1a, $t = 160 - 600 \text{ s}$).

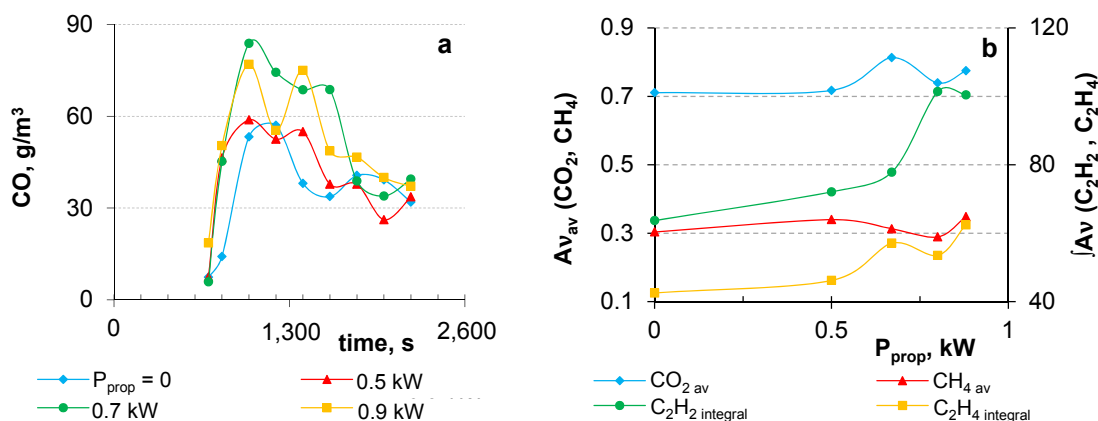


Figure 2: The effect of straw co-firing on the time- dependence variations of the CO formation (a) and the average values of volatile absorption intensity (b).

The variations of the straw thermal decomposition by increasing the additional heat input at co-firing of straw with propane determine the complex variations of the main combustion characteristics promoting the growth of the flame temperature and heat power of the device (Figure 3a, 3b). As follows from Figure 3, the dominant variations of the main flame characteristics occur during the primary stage of flame formation ($t < 600 \text{ s}$), when the flame temperature increases from 960 K up 1,250 K, whereas the heat power at this stage increases from 0.19 kW up to 0.44 kW. Besides, the co-firing of straw with propane demonstrates the influence on the flow dynamics increasing the average value of the flow axial velocity from 0.3 up to 0.62 m/s while decreasing the swirl intensity and swirl number of the secondary airflow from 1.2 to 0.8. Considering the effect of the additional heat input on the flow dynamics, one suggests that the additional heat input by propane flame enhances the downstream convective heat transport and partially restricts the reverse swirl flow formation, gradually decreasing the reverse heat transfer up to the surface of the biomass layer and the thermal decomposition of straw. This is confirmed by the measurements of the average values of the weight loss rate during the self-sustaining burnout of volatiles, when increasing of the additional heat input into the device above 0.5 kW results in a decrease of the weight loss rate of straw (Figure 1a).

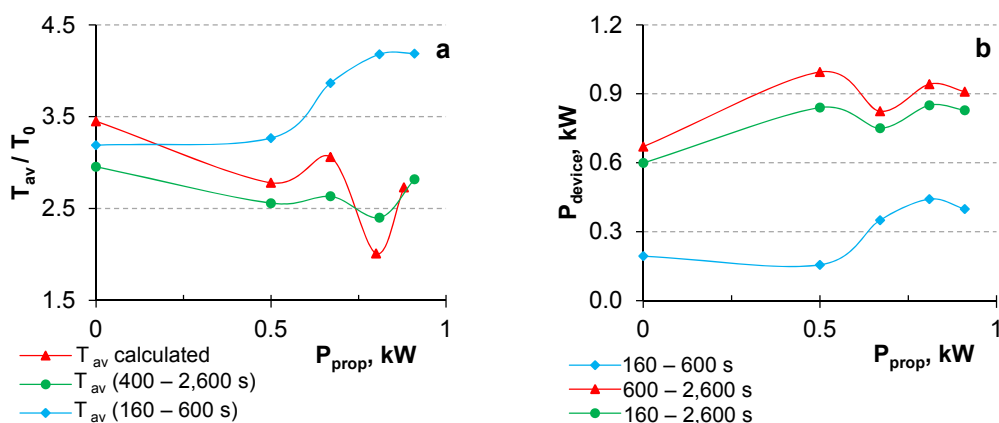


Figure 3: The effect of additional heat input on the flame temperature (a) and on the heat power of the device (b) when co-firing straw with propane.

The enhanced burnout of volatiles during the straw co-firing is also confirmed by variations of the products composition at the output of the device, determining the increase of the volumes fraction of CO₂ emission with the correlating decrease of the CO and H₂ mass fraction in the flue gas (Figure 4a, 4b). Moreover, the enhanced release of the combustible volatiles at the thermal decomposition of straw results in decrease of the air excess ratio in the flame reaction zone and in the products (Figure 4a), improving thus the combustion characteristics. Besides, the increase of the additional heat input into the device at straw co-firing results in decrease of the NO_x mass fraction in the products from 400 ppm to 240 ppm, indicating a cleaner and more efficient heat energy production.

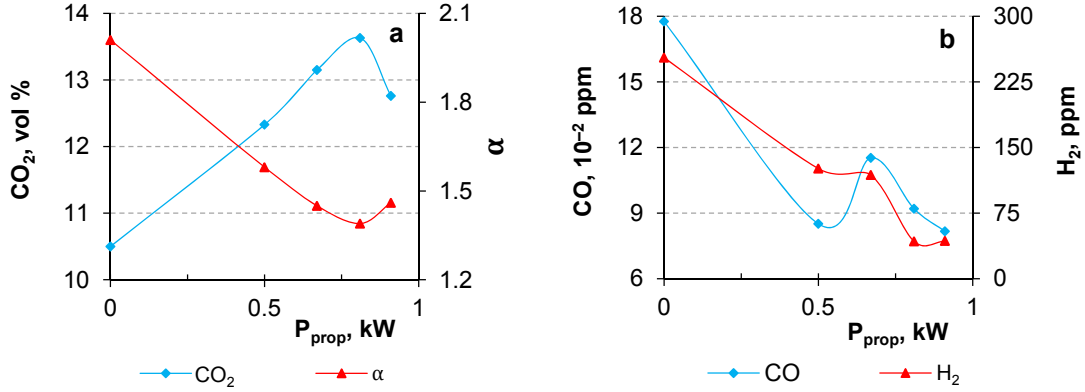


Figure 4: The variations of the flue gas composition providing the additional heat input into the straw combustion chamber by propane flame flow.

4. Results of mathematical modelling and numerical simulation

The mathematical model of the CO, H₂ combustion downstream the combustor was developed using MATLAB, considering the variations in CO/H₂ supply into the combustor and varying the propane flame flow input with account of the two second order exothermic gas phase reactions:



The variations of the molar fractions of six chemical species downstream the combustor were considered $\text{H}_2 = \text{M}_1$, $\text{OH} = \text{M}_2$, $\text{H}_2\text{O} = \text{M}_3$, $\text{H} = \text{M}_4$, $\text{CO} = \text{M}_5$, $\text{CO}_2 = \text{M}_6$. $E_1 = 14,965.2$ and $E_2 = 29,930.4$ J/mol are the activation energies of reactions Eq(1, 2); $A'_1 = 22$ and $A'_2 = 15,000$ m³/(mol·s) are the reaction-rate pre-exponential factors (Westley, 1980).

The input data for the simulation taken from the physical experiment at different amounts of biogas supply into the combustor is represented at Table 1.

Table 1: Input data of the average values of the molar density of the combustible volatiles (H₂ and CO) for numerical simulation by varying the propane supply into the combustor (q_{prop}).

q_{prop}	0 l/min	0.325 l/min	0.447 l/min	0.545 l/min	0.619 l/min
C'_1 (H ₂), mol/m ³	0.990	1.100	1.045	1.345	1.270
C'_5 (CO), mol/m ³	1.251	1.513	1.410	1.821	1.780

These values were used to describe the inlet conditions (decreasing the concentration values 4 times) of the combustion processes. At the inlet of the combustor, the mole fractions of the reactants H₂, OH and CO (C_k , $k = [1; 6]$) satisfy the condition $C_1 + C_2 + C_5 = 1$, whereas the mass fractions of the products H₂O, H and CO₂ – $C_3 = C_4 = C_6 = 0$. For 2D modelling, an axially symmetric ideal, laminar, compressible swirling flow in a coaxial cylindrical pipe (radius $R_0 = 0.05$ m, length $Z_0 = 0.1$ m), with the axial velocity $u = u_z/U_0$, radial velocity $u_r = u_r/U_0$, tangential velocity $w = u_\phi/V_0$, density ρ/ρ_0 , mass fraction C_k for eight species and temperature T/T_0 was calculated, considering the dependence on the time t , the axial $z = Z/R_0$ and radial r/R_0 coordinates, using MATLAB for the defined functions Eq(3-13). At the inlet $z = 0$, $U_0 = 0.1$ m/s, $V_0 = 3 \cdot U_0$, $\rho_0 = 1$ kg/m³, $T_0 = 300$ K, the scaled time t/t_0 ($t_0 = R_0/U_0 = 0.5$ s). Four Euler, temperature and six reaction-diffusion equations were considered to solve the problem. The perfect gas model $p = \rho T$ was used, where p is the dimensionless pressure. To describe the chemical reactions, the following parameters of Arrhenius kinetics were used (Smooke et al., 1987): $R = 8.314$ J/(mol·K) is the universal gas constant; $m_1 = 2$, $m_2 = 17$, $m_3 = 18$, $m_4 = 1$, m_5

= 28, $m_6 = 44 \text{ g/m}^3$ are the molecular weights of the species; $h_1 = 0$, $h_2 = 39.46$, $h_3 = -242$, $h_4 = 218$, $h_5 = -111$, $h_6 = -394 \text{ kJ/mol}$ are the enthalpies of the species, $c_p = 1,000 \text{ J/(kg}\cdot\text{K)}$ is the specific heat at constant pressure. For mathematical modelling, a PDE system of eleven equations was considered, describing the 2D compressible reacting swirling flow (four equations) and the heat with six diffusion-reaction equations in the following dimensionless form:

$$\partial \rho / \partial t + M(\rho) + \rho (\partial w / \partial z + r^{-1} \cdot \partial (r \cdot u) / \partial r) = 0 \quad (3)$$

$$\partial u_r / \partial t + M(u_r) - S \cdot v^2 / r^3 = -\rho^{-1} \partial \rho / \partial r + \text{Re}^{-1} \cdot (\Delta u_r - u_r / r^2) \quad (4)$$

$$\partial u / \partial t + M(u) = -\rho^{-1} \cdot \partial \rho / \partial z + \text{Re}^{-1} \cdot \Delta u \quad (5)$$

$$\partial w / \partial t + M(w) = \text{Re}^{-1} \cdot (\partial^2 w / \partial z^2 + r \cdot \partial / \partial r \cdot (r^{-1} \cdot \partial q / \partial w)) \quad (6)$$

$$\partial T / \partial t + M(T) = P_0 \cdot \rho^{-1} \cdot \Delta T + q_1 \cdot S_1 + q_2 \cdot S_2 \quad (7)$$

$$\partial C_i / \partial t + M(C_i) = P_i \cdot \Delta C_i + a_i \cdot m_i \cdot S_1 / m_1, \text{ where } i = 1 \text{ or } 3, a_1 = -1, a_3 = 1 \quad (8-9)$$

$$\partial C_i / \partial t + M(C_i) = P_i \cdot \Delta C_i + a_i \cdot m_i \cdot S_1 / m_1 + a_i \cdot m_i \cdot S_2 / m_2, \text{ where } i = 2 \text{ or } 4, a_2 = -1, a_4 = 1 \quad (10-11)$$

$$\partial C_i / \partial t + M(C_i) = P_i \cdot \Delta C_i + a_i \cdot m_i \cdot S_2 / m_2, i = 5 \text{ or } 6, \text{ where } a_5 = -1, a_6 = 1 \quad (12-13)$$

where $M(q) = u \cdot \partial q / \partial z + u_r \cdot \partial q / \partial r$, $\Delta q = \partial^2 q / \partial z^2 + r^{-1} \partial / \partial r (r \partial q / \partial r)$ are the convective and diffusion terms, $S_1 = \rho \cdot A_1 \cdot C_1 \cdot C_2 \cdot \exp(-\delta_1 / T)$, $S_2 = \rho \cdot A_2 \cdot C_2 \cdot C_5 \cdot \exp(-\delta_2 / T)$ are the chemical source terms, $P_k = D_k / (U_0 r_0) = 0.01$, $k = [1; 6]$, $P_0 = \lambda / (c_p \cdot \rho_0 \cdot U_0 \cdot r_0) = 0.05$, $q_1 = Q_1 / (c_p T_0) = 124.9$, $q_2 = 9.42$, $Q_1 = (m_1 \cdot h_1 + m_2 \cdot h_2 - m_3 \cdot h_3 - m_4 \cdot h_4) / (m_1 \cdot m)$, $Q_2 = (m_2 \cdot h_2 - m_4 \cdot h_4 + m_5 \cdot h_5 - m_6 \cdot h_6) / (m_2 \cdot m)$ expressed in J/kg are the heat effects of each reaction, $\delta_k = E_k / (R \cdot T_0)$, ($\delta_1 = 6.0$, $\delta_2 = 12.0$) are the scaled activation energies, $\lambda = 2.5 \cdot 10^{-1} \text{ W/(m}\cdot\text{K)}$ is the thermal conductivity, $D_k = 2.510^{-4} \text{ m}^2/\text{s}$ is the molecular diffusivity of the species, $m = 18.3 \text{ g/m}^3$ is the averaged value of the molecular weights of the species. $A_1 = A_1' \rho_0 r_0 / (U_0 m_2) = 647.1$, $A_2 = A_2' \rho_0 r_0 / (U_0 m_5) = 2.7 \cdot 10^5$ are the scaled reaction-rate pre-exponential factors, $S = u_0 / w_0 = 3$ is the swirl number, $\text{Re} = U_0 r_0 \rho_0 / \mu = 10,000$ is the Reynolds number, $\mu = 5 \cdot 10^{-7} \text{ kg/(m}\cdot\text{s)}$ is the viscosity.

The boundary of the pipe ($r = r_0$) is a subject to the heat loss modelled by Newtonian cooling to the ambient surroundings at a temperature T_0 and with the heat transfer coefficient $h = 0.1 \text{ J/(s}\cdot\text{m}^2\cdot\text{K)}$. The dimensionless boundary conditions are as mentioned in Kalis et al. (2018). To solve the discrete problem with the time step 0.0008, we use the ADI method (Kalis et al., 2018) in the vector form of eleven functions in Eq(3 – 13). The numerical results depending on (z , r , t) were obtained at $0 < z < 2$; $0 < r < 1$; $0 < t < 1$.

Regarding the mechanism described by the chemical reactions Eq(1, 2), the maximum values of the temperature T_{\max} , flow component velocities $u_{r, \max}$, u_{\max} , mass fractions $C_{k, \text{end}}$ of the species $\text{CO}(C_5)$, $\text{H}_2(C_1)$, $\text{CO}_2(C_6)$, $\text{H}(C_4)$ and averaged temperatures T_{av} are summarized in Table 2. The maximum value of H, CO_2 , u_{\max} , T_{\max} , T_{av} , $u_{r, \max}$ and the minimum value of CO were obtained for the first three regimes of the propane flame flow. The mass fraction for $\text{H}_2(C_1)$ decreased by about 0.040 and was almost constant for all the series. The mass fraction of the reactant $\text{OH}(C_2)$ decreased to zero at $t = t_f = 0.5 \text{ s}$. The variations of the T_{\max} , $u_{r, \max}$, u_{\max} and CO_2 mass fractions during the straw co-firing with propane correlate with the results of the experimental study (Figures 3a, 4a).

Table 2: Numerical simulation of the values of the mass fractions of chemical species ($C_{k, \text{end}}$), maximum (T_{\max}) and average (T_{av}) flame temperature, maximum axial (u_{\max}) and radial ($u_{r, \max}$) flow velocities versus the variation of the biogas supply rate into the combustor ($t_{\text{end}} = 0.5 \text{ s}$; $C_{2, \text{end}} = 0$).

Species	0 l/min	0.325 l/min	0.447 l/min	0.545 l/min	0.619 l/min
$C_{1, \text{start}}^{(\text{H}_2)}$	0.25	0.28	0.26	0.34	0.32
$C_{5, \text{start}}^{(\text{CO})}$	0.31	0.37	0.35	0.46	0.45
$C_{2, \text{start}}^{(\text{OH})}$	0.44	0.35	0.39	0.20	0.23
$C_{1, \text{end}}$	0.209	0.243	0.222	0.299	0.282
$C_{5, \text{end}}$	0.002	0.027	0.028	0.235	0.185
$C_{3, \text{end}}^{(\text{H}_2\text{O})}$	0.268	0.150	0.194	0.072	0.078
$C_{4, \text{end}}^{(\text{H})}$	0.026	0.026	0.023	0.012	0.013
$C_{6, \text{end}}^{(\text{CO}_2)}$	0.485	0.539	0.536	0.354	0.416
u_{\max}	4.63	4.14	4.35	3.48	3.60
$u_{r, \max}$	2.60	2.52	2.53	2.50	2.51
T_{\max}	3.71	2.98	3.28	2.62	2.26
T_{av}	3.45	2.78	3.06	2.01	2.73

5. Conclusions

The complex measurements of the thermal decomposition of straw and combustion of volatiles during the co-firing of straw with propane give evidence that the co-firing of straw assures the enhanced thermal decomposition of straw pellets (by about 25 – 50 %) with the enhanced input of volatiles into the combustor at the primary pre-combustion stage (up to ~25 %), which improves the heat production in the reaction zone and increases the flame temperature at the primary flame formation stage, thus enhancing the ignition of the biomass and increasing the produced heat energy per mass of burned solid fuel. The improvement of the combustion conditions correlates with the improvement of the products composition almost by half decreasing the mass fraction of the polluting CO and NO_x emissions in the flue gas.

The results of the mathematical modelling confirm that, in accordance with the results of the experimental study, the co-firing of straw with propane advances the decrease of the average values of the flame temperature at the self-sustaining combustion stage, which in the experimental work is described by the variations of the flame flow dynamics caused by a cross flow of the propane flame. However, the decrease of the temperature, axial flow velocity and of the mass fractions of the main combustion products (CO₂, H₂O) indicates the incomplete combustion of the volatiles (CO and H₂) along the pipe. Upon analyzing the obtained numerical results of the mathematical modelling, it is suggested that more factors should be accounted in for the mathematical model to improve the numerical results and to make them more applicable to the simulation of experimental results.

Acknowledgments

The authors would like to acknowledge the financial support from the European Regional funding of project No. 1.1.1.1/16/A/004.

References

- Agbor E.U., 2015, Biomass Co-firing with Coal and Natural Gas, Master's thesis, University of Alberta, Department of Mechanical Engineering, Alberta, Canada.
- Barmina I., Kolmickovs A., Valdmanis R., Zake M., Kalis H., Strautins U., 2018a, Experimental Study and Mathematical Modelling of Straw Co-Firing with Peat, *Chemical Engineering Transactions*, 65, 91–96.
- Barmina I., Valdmanis R., Zake M., 2018b, The Effects of Biomass Co-Gasification and Co-Firing on The Development of Combustion Dynamics, *Energy*, 146, 4–12.
- Basu, P., 2018, Biomass Combustion and Cofiring. Biomass Gasification, Chapter In: Pyrolysis and Torrefaction (3rd Ed), Academic Press, Elsevier BV, Canada, 393–413.
- EU Commision, 2030 -climate&energy framework https://ec.europa.eu/clima/policies/strategies/2030_en
- Jandacka J., Holubcik M., Papucik S, Nosek R., 2012, Combustion of Pellets from Wheat Straw, *Acta Montanistica Slovaca*, 17 (4), 283–289.
- Kalis H., Marinaki M., Strautins U., 2018, The Numerical Simulation of Electromagnetic Field Effects in the Combustion Process, *Mathematical Modelling and Analysis*, 23 (2), 327–343
- Nordgren D., Hedman H., Padban N., Boström D., Öhman M., 2013, Ash Transformation in Pulverized Fuel Co-Combustion of Straw and Woody Biomass, *Fuel Processing Technology*, 105, 52–58.
- Nussbaumer T., 2003, Combustion and Co-Combustion of Biomass: Fundamental, Technologies, and Primary Measures for Emission Reduction, *Energy & Fuels*, 17, 1510–1521.
- Smooke M.D., Turnbull A.A., Mitchell R.E., Keyes D.E., 1988, Solution of Two-Dimensional Axisymmetric Laminar Diffusion Flames by Adaptive Boundary Value Methods, *Proceedings of the NATO Advanced Research Workshop on "Mathematical Modelling in Combustion and Related Topics"*, Lyon, France, NATO ASI Series (Ed.), Applied Sciences, 140, 261–300.
- Vasilev S., Baxter D., Andersen L.K., Vasileva C.G., Morgan T.J., 2012, An Overview of The Organic and Inorganic Phase Composition of Biomass, *Fuel*, 94, 1–33.
- Veijonen K., Vainikka P., Järvinen T., Alakangas E., 2003, Biomass Co-Firing – an Efficient Way to Reduce Greenhouse Gas Emissions, EUBIONET – European Bioenergy networks, Finland, <ec.europa.eu/energy/sites/ener/files/documents/2003_cofiring_eu_bionet.pdf> accessed 16.01.2019.
- Wang X., Hu Z., Deng Sh., Wiong Y., Tan H., 2014, Effect of Biomass/Coal Co-Firing and Air Staging on NO_x Emission and Combustion Efficiency in a Drop Tube Furnace, *Energy Procedia*, 61, 2331–2334.
- Westley F., 1980, Table of Recommended Rate Constants for Chemical Reactions Occurring in Combustion, National Bureau of Standards, Chemical kinetics information Centre, Washington DC, USA.
- Yang H., Yan R., Chen H., Lee D.H., Zheng C.H., 2007, Characteristics of Hemicellulose, Cellulose and Lignin Pyrolysis, *Fuel*, 86, 1781–1788.